

Catalytic growth of N-doped MgO on Mo(001)

Martin Grob,* Marco Pratzler, and Markus Morgenstern

II. Institute of Physics B and JARA-FIT, RWTH Aachen University, D-52074 Aachen, Germany

Marjana Ležaić

Peter-Grünberg Institute, Forschungszentrum Jülich and JARA, D-52425 Jülich, Germany

(Received 21 February 2012; revised manuscript received 18 July 2012; published 24 August 2012)

A simple pathway to grow thin films of N-doped MgO (MgO:N), which has been found experimentally to be a ferromagnetic d^0 insulator, is presented. It relies on the catalytic properties of a Mo(001) substrate using the growth of Mg in a mixed atmosphere of O_2 and N_2 . Scanning tunneling spectroscopy reveals that the films are insulating and exhibit an N-induced state slightly below the conduction band minimum.

DOI: [10.1103/PhysRevB.86.075455](https://doi.org/10.1103/PhysRevB.86.075455)

PACS number(s): 68.55.aj, 68.37.Ef, 81.15.Hi

I. INTRODUCTION

Recently, it has been found that MgO:N-films grown by molecular beam epitaxy (MBE) exhibit ferromagnetism after being annealed at 1020 K.¹ The optimized N concentration was 2.2% exhibiting coercive fields as large as 60 mT at $T = 10$ K and magnetic moments per N atom of $0.3 \mu_B$ barely reducing up to room temperature. A Curie temperature $T_C \simeq 550$ K has been extrapolated and indications that N is incorporated substitutionally on the O site have been deduced from core level spectroscopy. Moreover, independent studies of N implantation (80 keV) into MgO has led to a hysteresis with a coercive field of 30 mT at 300 K.² This raises hope that reliable d^0 ferromagnetism avoiding d metals can be realized in MgO:N at $T = 300$ K. Such magnetism without d orbitals has previously been found in thin films of undoped oxides³ including MgO (Ref. 4) or defective carbon systems,⁵ however, with limited control since relying on defects. ZnO with sp -type dopants such as C, N, B, Li, Na, Mg, Al, and Ga shows ferromagnetic signals, too,^{6,7} but, likely, Zn or O vacancies and Zn d orbitals are involved in the magnetic coupling.^{6,8}

The d^0 ferromagnetism has been proposed theoretically relying on the double exchange mechanism in narrow impurity bands.⁹ But the high T_C proposed originally has been challenged by going beyond the mean-field approximation¹⁰ or by considering correlation effects.^{11–13} Partly, even the absence of ferromagnetism has been found.¹¹ This renders the high T_C observed experimentally in obvious disagreement with current theory and suggests more detailed studies are needed.

MgO:N films, in addition, exhibit bipolar resistive switching behavior¹⁴ prior to annealing. Resistance contrasts as large as 4 orders of magnitude, switching currents as low as 100 nA, and switching times into both states below 10 ns have been obtained.¹ This makes MgO:N also interesting for nonvolatile memories. However, the incorporation of N into MgO is difficult due to the strongly endothermic incorporation of N atoms with respect to N_2 (energy cost per N atom: 10 eV).¹⁵ It requires, for example, atomic beams of N and O produced by a high-frequency ion plasma source¹ or N^+ implantation.² Here, we demonstrate a simplified pathway using the catalytic abilities of a Mo(001) substrate. Thus, we establish a model system of MgO:N for surface science. Mo(001) is chosen since thin MgO films of high quality can be grown epitaxially due to the relatively small lattice

mismatch of 6%.^{16–18} Moreover, catalytic properties of Mo with respect to N_2 are known, for example, nitrogenase within bacteria using molybdenum enzymes as catalyst.¹⁹ Catalytic N_2 dissociation on surfaces has been induced successfully for the electronically similar W(001), whereas growth properties of MgO are, however, unknown.^{20–22} We have grown thin films of MgO:N on Mo(001) with thicknesses up to 10 monolayers (ML) at optimal doping. Scanning tunneling spectroscopy (STS) has revealed that the Fermi level is well within the band gap, indicating an insulating behavior of the film. Moreover, an unoccupied state close to the conduction band has been found, which is not present in pure MgO films.

II. RESULTS AND DISCUSSION

The experiments are performed in an ultrahigh vacuum at a base pressure of $p = 5 \times 10^{-11}$ mbar. First, the Mo(100) crystal was cleaned by cyclically annealing within O_2 at an initial pressure of $p_{O_2} = 5 \times 10^{-7}$ mbar and 1400 K, followed by flashing to 2300 K.²³ After every cycle, p_{O_2} is slightly reduced. The MgO:N films are prepared by molecular beam epitaxy of magnesium at $p_{O_2} = 1 \times 10^{-7}$ mbar and N_2 pressure $p_{N_2} = 5 \times 10^{-6}$ mbar. The deposition temperature T_D is 300 K, if not given explicitly. The deposition rate of Mg controlled by a quartz microbalance is 0.5 ML/min. After MgO:N deposition, the samples are annealed at 1100 K for 10 min. Figure 1(a) shows a scanning tunneling microscopy (STM) image of 7 ML $MgO_{0.973}N_{0.027}$. It exhibits islands on top of a MgO:N wetting layer. From comparison of the coverage determined by the quartz balance and the volume of the MgO:N islands, we estimate the wetting layer thickness to be 1–2 ML. Such relatively rough films are occasionally also observed in pure MgO films. So far, we have not been able to prepare films of similar smoothness as, for example, in Fig. 1 of Ref. 18 for MgO:N. More studies are required to attribute the different morphologies to intrinsic properties of MgO and MgO:N. Thicker samples exhibit a plain surface with corrugations below 0.5 nm as measured for a film with a thickness of 40 ML by atomic force microscopy (AFM) and shown in Fig. 1(c). We check the crystalline quality and chemical purity of Mo(100) and the MgO:N films by low-energy electron diffraction (LEED) and Auger electron spectroscopy (AES). A complete AES spectrum at a primary

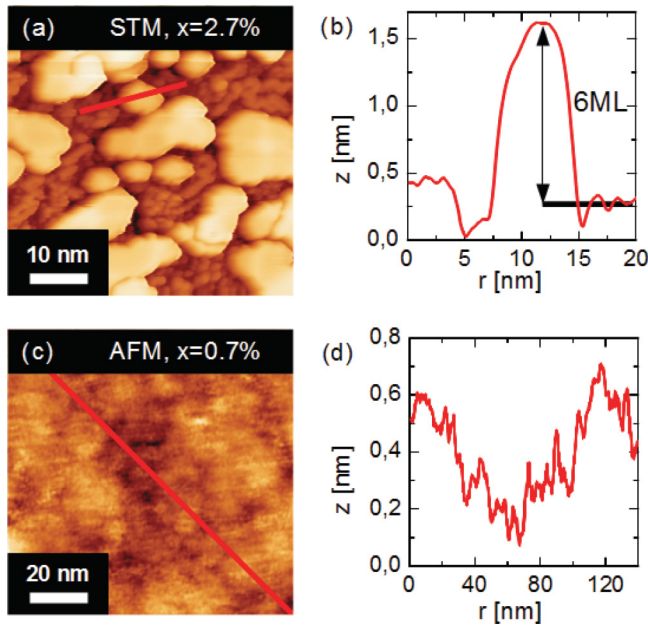


FIG. 1. (Color online) (a) STM image of 7 ML $\text{MgO}_{0.973}\text{N}_{0.027}$ film on Mo(001) with thicker islands (bright areas) on top of a wetting layer of 1–2 ML; $(50 \times 50) \text{ nm}^2$, $U = 3 \text{ V}$, $I = 0.5 \text{ nA}$. (b) Line profile along the red line marked in panel (a) with the height of the island above the wetting layer marked. (c) Tapping mode AFM image of 40 ML $\text{MgO}_{0.993}\text{N}_{0.007}$ film on Mo(001) after transfer into an ambient environment; $(100 \times 100) \text{ nm}^2$, $f = 281 \text{ kHz}$, free amplitude $A = 30 \text{ nm}$, setpoint 60%. (d) Line profile along the red line marked in panel (c).

electron energy of 1 keV sensitive to the upper 2 nm (9 to 10 ML)²⁴ is shown in Fig. 2(a). Next to the O peak and the N peak there is a small amount of Mo which remains constant independent of the number of MgO:N layers. The nominal atomic concentration x_i of element i within homogeneous films is calculated from the AES peak height Y_i shown in Fig. 2(b) according to²⁵

$$x_i = \frac{Y_i/S_i}{\sum_a Y_a/S_a}, \quad (1)$$

where S_i denotes the normalized sensitivity factor for element i and a sums over all relevant elements. For Mo this results in $x = 4.5\%$ relating to O. We believe that this thickness-independent amount originates from the Mo sample holder due to an imperfect focusing of the electron beam onto the sample.

The N concentration x depends on the deposition temperature T_D as shown in Fig. 2(c) for a 7-ML MgO:N film. Up to $x = 6\%$ is achieved at $T_D = 850 \text{ K}$, indicating a more effective dissociation of N_2 at higher T_D . Notice that $x = 6\%$ at 7 ML is still far below the amount of N expected from a full N coverage of Mo(001). Next, we prepare MgO:N films with a thickness of up to 100 ML at $T_D = 900 \text{ K}$. The nitrogen amount within the MgO:N decreases with film thickness as shown in Fig. 3. A 60-ML-thick MgO:N film contains only 0.3% nitrogen in comparison to 3.2% at a thickness of 7 ML. Assuming homogeneous distribution of N, this implies that the total amount of N in both films is roughly the same,

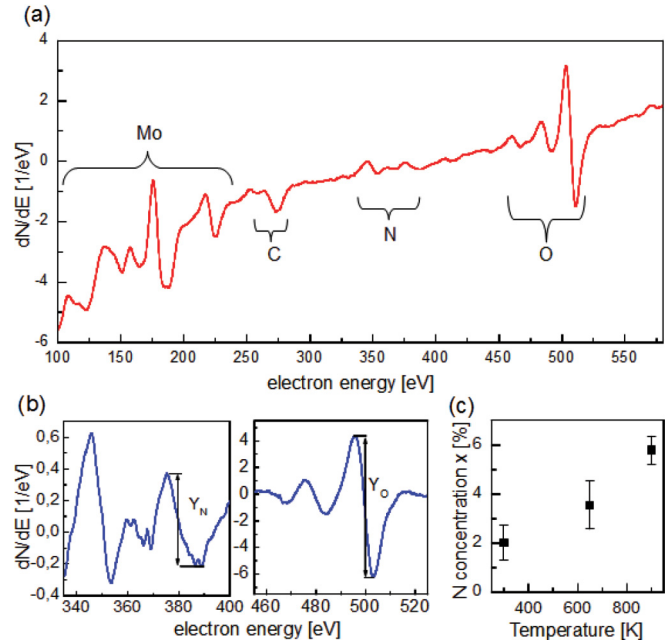


FIG. 2. (Color online) (a) Differential AES spectra of 7 ML $\text{MgO}_{0.979}\text{N}_{0.031}$ with assignment of the peaks different elements recorded at a primary energy of $E = 1 \text{ keV}$. Above the O peak, there is no other peak related to another element. (b) Higher resolution spectra from panel (a) of N and O with the corresponding peak-to-peak height Y_i marked. (c) Nitrogen concentration x of 7-ML-thick MgO:N films as a function of the deposition temperature T_D .

evidencing that N_2 is dissociated on the Mo(100) surface only. We assume that, during MgO growth or annealing, the atomic N from the surface is incorporated into the MgO film. To

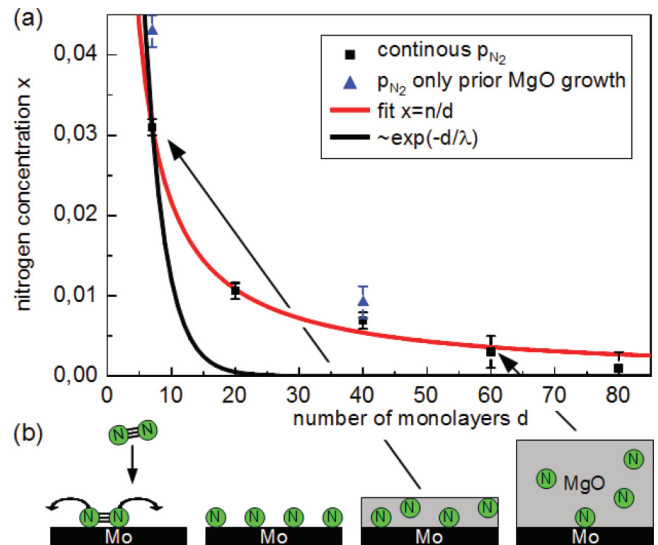


FIG. 3. (Color online) (a) Nitrogen concentration x as a function of monolayers d . Different symbols mark different preparation methods, the red fit curve assumes a constant amount of N atoms homogeneously distributed within the MgO film, and the black curve assumes the same amount of N at the Mo/MgO interface only (see text). (b) Sketch of N_2 incorporation. Left: N_2 dissociation on Mo(001). Right: Incorporation of N into MgO leaving the amount of N independent of the MgO thickness.

support this scenario, we fit the data assuming a constant areal concentration n of N atoms:

$$x = \frac{n}{d}, \quad (2)$$

where d denotes the number of MgO ML and n represents the concentration of N atoms with respect to the sum of N and O atoms if only one ML is prepared. If we assume that all N atoms are substitutionally incorporated into the first monolayer of MgO:N, the red fit curve plotted in Fig. 3(a) shows excellent agreement with the measured data points using $n = 21.6\%$. Assuming interstitial impurities, i.e., dumbbells of NO,¹⁵ Eq. (2) has to be slightly modified and results in $n = 18.2\%$.

The resulting Auger current I of the N peak at 379 eV can be calculated, assuming a homogeneous distribution of N in the sample resulting in a N concentration per layer proportional to $1/z$, with z being the film thickness. The amount of incoming electrons with $E = 1$ keV decays exponentially, as well as the amount of Auger electrons leaving the sample. This results in

$$I = \frac{I_0}{z} \int_0^z e^{-z'/\lambda_1} e^{-z'/\lambda_2} dz' = \frac{I_0}{az} (1 - e^{-az}),$$

$$a = \frac{\lambda_1 + \lambda_2}{\lambda_1 \lambda_2}, \quad (3)$$

with I_0 being a constant depending on the details of the experiment. One finds an exponential part multiplied by the dominating $1/z$ part. Using the experimentally verified mean free path of $\lambda_1(1 \text{ keV}) = 2 \text{ nm}$ and $\lambda_2(379 \text{ eV}) = 1 \text{ nm}$,²⁴ we obtain a decrease in the signal by a factor of 5 from 7 to 40 ML, which agrees well with our measurements. This is shown by the red curve in Fig. 3(a), which has been adapted to the experimental point at $x = 0.031$ to get rid of the unknown I_0 .

Nearly the same n can be achieved by another preparation method: Prior to the deposition of Mg in a pure O₂ environment, we expose the Mo crystal to N₂ ($p = 5 \times 10^{-6}$ mbar) at 300 K for 10 min. Afterwards, we grow MgO without N₂ at $T = 900 \text{ K}$, leading to very similar N concentrations as shown by the blue triangles in Fig. 3(a). Thus, obviously, the dissociation of N₂ takes place at Mo(001) only. Finally, a third preparation is performed: 10 ML of pristine MgO are grown first at $p_{\text{N}_2} < 10^{-11}$ mbar. Subsequently, 10 ML MgO:N are deposited at $T_D = 300 \text{ K}$ and $p_{\text{N}_2} = 5 \times 10^{-6}$ mbar. No nitrogen is found in the sample, i.e., $x < 0.2\%$, which has to be compared to the $x = 3.1\%$ obtained for 7-ML MgO:N grown under identical conditions directly on the substrate. Thus, if Mo is covered by MgO, the catalytic effect of the substrate is inhibited. In order to show that the N is incorporated into the MgO film and does not reside on the substrate, we also calculate the expected AES signal of N for this case assuming a maximum concentration of $n = 28\%$ at the Mo/MgO interface, i.e., adapting the curve to the 3.1% data point in Fig. 3(a). This results in

$$I = I_0 e^{-z/\lambda_1} e^{-z/\lambda_2}. \quad (4)$$

The results are plotted in Fig. 3(a), too, revealing a strong discrepancy with the experimental data. In particular, the strength of x at $d = 40 \text{ ML}$ is 10^{-6} , while the experimental value is 0.69%. Figures 1(c) and 1(d), which have been

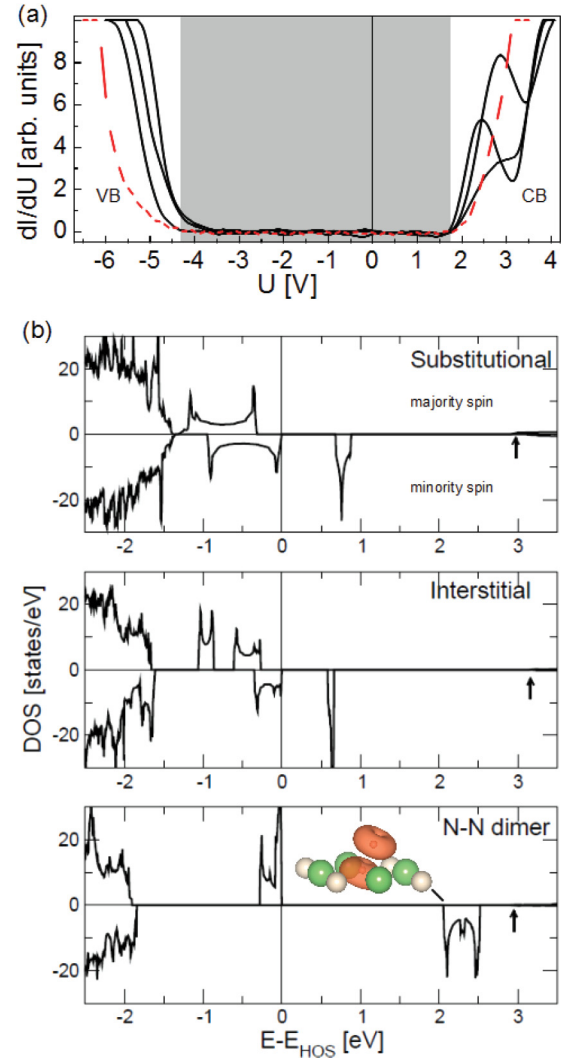


FIG. 4. (Color online) (a) $dI/dU(U)$ spectra measured by STS on an 11-ML-high MgO_{0.96}N_{0.04} island ($U_{\text{stab}} = 3 \text{ V}$, $I_{\text{stab}} = 0.5 \text{ nA}$, $U_{\text{mod}} = 40 \text{ mV}$) at several positions (straight lines) and on an 11-ML-thick pristine MgO island (dashed line). The average film thickness in both cases is 7 ML. (b) Calculated density of states (DOS) for substitutional and interstitial impurity as well as a N-N dimer at MgO surface. HOS: Highest occupied state. All states between -1.2 eV and 3 eV are N induced; CBM is marked by an arrow. The inset shows the calculated charge density of the unoccupied N-induced states of a N-N dimer at the surface. The large green and small white spheres show Mg and O, respectively.

recorded on a 40-ML MgO film exhibiting an AES signal of $x = 0.7\%$, confirm that the MgO thickness is rather homogeneous (roughness $\sigma = 150 \text{ pm}$), making it impossible that N at the interface could have been detected by AES. Thus, we conclude that N dissociated at the Mo(001) is incorporated into the MgO film, but we do not know the incorporation site. To tackle this question, we perform *in situ* STS, which probes the local density of states at the surface. Figure 4 compares the STS curves of 11-ML films of MgO_{0.96}N_{0.04} and undoped MgO.¹⁸ Doping by N leads to a shift of the Fermi level E_F towards the valence band by about 1 eV. The fact that this shift is smaller than expected for p -type doping by N is possibly due to donation of

electrons, accomplished by the Mo substrate.²⁶ An additional peak with a maximum at 0.3 eV below the conduction band minimum (CBM) appears after N doping. This is observed for three different N concentrations, i.e., MgO thicknesses. The peak energy varies laterally by ± 0.3 eV. Density functional theory (DFT) calculations of bulk MgO with substitutional N predict occupied p levels close to the valence band maximum (VBM) and an unoccupied, spin polarized level within the middle of the band gap, if self interaction correction is included.^{11,12}

This disagrees with our experiment. Since surfaces were not included in these calculations, we performed first-principles DFT calculations including the surface within the spin-polarized generalized gradient approximation²⁷ using projector augmented-wave potentials as implemented in the Vienna *Ab initio* Simulation Package (VASP).²⁸ Correlation effects on the p shells of N dopants were accounted for by the DFT + U scheme in Dudarev *et al.*'s approach²⁹ with an on-site effective Coulomb parameter, $U_{\text{eff}} = 3.4$ eV. A kinetic energy cutoff of 500 eV and a $6 \times 6 \times 1$ Γ -centered k -point mesh was used. The supercell consists of nine atomic layers MgO(001) using the experimental lattice parameter and a 16-Å-thick layer of vacuum. All atomic positions as well as the thickness of the MgO slab were fully relaxed.

Three different configurations with N atoms in the surface layer were calculated: (i) one N-atom substituting an oxygen, (ii) one N-atom at the interstitial site, and (iii) an N-N dimer with one N atom being substitutional and the other at the nearest interstitial site. In case (ii), the calculation was initiated

with N at the interstitial site, but the system relaxed to a configuration where N and O exchanged their places, i.e., N ended up substitutionally and O interstitially. However, the N-derived p states for cases (i) and (ii) were found within 2.2 eV above the VBM, very similar to the MgO bulk^{11,12} as shown in Fig. 4(b) in the first two panels exhibiting no peaks close to the CBM. We also tried a more complex N structure as, e.g., the N-N dimer at the surface shown in Fig. 4(b), lowest panel, and exhibiting unoccupied N-type p states close to the CBM. However, there is another peak of similar geometric intensity distribution in the center of the band gap not observed in the experiment. Thus, even more complex structures might be responsible for the observed peak.

III. CONCLUSION

In conclusion, we prepared thin films of N-doped MgO with an N concentration up to 6% by using the catalytic effect of Mo(001) for N₂ dissociation. Compared with pristine MgO, an additional state close to the conduction band minimum was observed by STS which could not be attributed to simple N impurity configurations.

ACKNOWLEDGMENTS

Helpful discussions with P. Mavropoulos, S. Blügel and S. Parkin as well as financial support from the DFG under Grant No. SFB 917-A3 and the HGF-YIG under Grant No. VH-NG-409 are gratefully acknowledged.

*Corresponding author: grob@physik.rwth-aachen.de

¹C. H. Yang, Ph. D. thesis, Stanford University, Stanford, CA, 2010.

²L. Chun-Ming, G. Hai-Quan, X. Xia, Z. Yan, J. Yong, C. Meng, and Z. Xiao-Tao, *Chin. Phys. B* **20**, 047505 (2011).

³M. Ventakesan, C. B. Fitzgerald, and J. M. D. Coey, *Nature (London)* **430**, 630 (2004); J. M. D. Coey, M. Venkatesan, P. Stamenov, C. B. Fitzgerald, and L. S. Dorneles, *Phys. Rev. B* **72**, 024450 (2005); M. Khalid *et al.*, *ibid.* **80**, 035331 (2009); N. H. Hong, J. Sakai, N. Poirrot, and V. Brizé, *ibid.* **73**, 132404 (2006); D. Gao, J. Li, Z. Li, Z. Zhang, J. Zhang, H. Shi, and D. Xue, *J. Phys. Chem. C* **114**, 11703 (2010).

⁴C. M. Araujo *et al.*, *Appl. Phys. Lett.* **96**, 232505 (2010); C. Martinez-Boubeta, J. I. Beltran, L. Balcells, Z. Konstantinovic, S. Valencia, D. Schmitz, J. Arbiol, S. Estrade, J. Cornil, and B. Martinez, *Phys. Rev. B* **82**, 024405 (2010).

⁵P. Esquinazi, D. Spemann, R. Hohne, A. Setzer, K. H. Han, and T. Butz, *Phys. Rev. Lett.* **91**, 227201 (2003); S. Talapatra, P. G. Ganesan, T. Kim, R. Vajtai, M. Huang, M. Shima, G. Ramanath, D. Srivastava, S. C. Deevi, and P. M. Ajayan, *ibid.* **95**, 097201 (2005).

⁶H. Pan, J. B. Yi, L. Shen, R. Q. Wu, J. H. Yang, J. Y. Lin, Y. P. Feng, J. Ding, L. H. Van, and J. H. Yin, *Phys. Rev. Lett.* **99**, 127201 (2007).

⁷C.-F. Yu, T.-J. Lin, S.-J. Sun, and H. Chou, *J. Phys. D: Appl. Phys.* **40**, 6497 (2007); S. Chawla, K. Jayanthi, and R. K. Kotnala, *Phys. Rev. B* **79**, 125204 (2009); *J. Appl. Phys.* **106**, 113923 (2009); Y. Ma *et al.*, *IEEE Trans. Magn.* **46**, 1338 (2010).

⁸X. L. Li *et al.*, *IEEE Trans. Magn.* **46**, 1382 (2010); X. G. Xu *et al.*, *Appl. Phys. Lett.* **97**, 232502 (2010); J. B. Yi *et al.*, *Phys. Rev. Lett.* **104**, 137201 (2010); D. Gao *et al.*, *J. Phys. Chem. C* **114**, 13477 (2010); V. Bhosle and J. Narayan, *Appl. Phys. Lett.* **93**, 021912 (2008).

⁹I. S. Elfimov, S. Yunoki, and G. A. Sawatzky, *Phys. Rev. Lett.* **89**, 216403 (2002); K. Kenmochi *et al.*, *Jpn. J. Appl. Phys.* **43**, L934 (2004); K. Kenmochi *et al.*, *J. Phys. Soc. Jpn.* **73**, 2952 (2004); V. A. Dinh *et al.*, *ibid.* **75**, 093705 (2006); I. S. Elfimov, A. Rusydi, S. I. Csiszar, Z. Hu, H. H. Hsieh, H. J. Lin, C. T. Chen, R. Liang, and G. A. Sawatzky, *Phys. Rev. Lett.* **98**, 137202 (2007).

¹⁰P. Mavropoulos, M. Ležaić, and S. Blügel, *Phys. Rev. B* **80**, 184403 (2009).

¹¹A. Droghetti, C. D. Pemmaraju, and S. Sanvito, *Phys. Rev. B* **78**, 140404 (2008); V. Pardo and W. E. Pickett, *ibid.* **78**, 134427 (2008); H. Wu, A. Stroppa, S. Sakong, S. Picozzi, M. Scheffler, and P. Kratzer, *Phys. Rev. Lett.* **105**, 267203 (2010).

¹²I. Slipukhina, P. Mavropoulos, S. Blügel, and M. Ležaić, *Phys. Rev. Lett.* **107**, 137203 (2011).

¹³B. Gu, N. Bulut, T. Ziman, and S. Maekawa, *Phys. Rev. B* **79**, 024407 (2009).

¹⁴R. Waser, R. Dittmann, G. Staikov, and K. Szot, *Adv. Mater.* **21**, 2632 (2009).

¹⁵M. Pesci, F. Gallino, C. Di Valentin, and G. Pacchioni, *J. Phys. Chem. C* **114**, 1350 (2010).

¹⁶M. C. Gallagher, M. S. Fyfield, L. A. Bumm, J. P. Cowin, and S. A. Joyce, *Thin Solid Films* **445**, 90 (2003).

- ¹⁷S. Benedetti, H. M. Benia, N. Nilius, S. Valeri, and H. J. Freund, *Chem. Phys. Lett.* **430**, 330 (2006).
- ¹⁸C. Pauly, M. Grob, M. Pezzotta, M. Prutzer, and M. Morgenstern, *Phys. Rev. B* **81**, 125446 (2010).
- ¹⁹J. Chatt, J. R. Dilworth, R. L. Richards, and J. R. Sanders, *Nature (London)* **224**, 1201 (1969).
- ²⁰M. Alducin, R. Díez Muiño, H. F. Busnengo, and A. Salin, *Phys. Rev. Lett.* **97**, 056102 (2006).
- ²¹L. R. Clavenna and L. D. Schmidt, *Surf. Sci.* **22**, 365 (1970).
- ²²C. T. Rettner, E. K. Schweizer, and H. Stein, *J. Chem. Phys.* **93**, 1442 (1990).
- ²³M. Bode, S. Krause, L. Berbil-Bautista, S. Heinze, and R. Wiesendanger, *Surf. Sci.* **601**, 3308 (2007).
- ²⁴A. Akkerman *et al.*, *Phys. Status Solidi B* **198**, 769 (1996).
- ²⁵S. Mroczkowski and D. Lichtmann, *J. Vac. Sci. Technol. A* **3**, 1860 (1985).
- ²⁶X. Shao, P. Myrach, N. Nilius, H. J. Freund, U. Martinez, S. Prada, L. Giordano, and G. Pacchioni, *Phys. Rev. B* **83**, 245407 (2011).
- ²⁷J. P. Perdew, K. Burke, and M. Ernzerhof, *Phys. Rev. Lett.* **77**, 3865 (1996).
- ²⁸G. Kresse and J. Hafner, *Phys. Rev. B* **47**, 558 (1993); G. Kresse and J. Furthmüller, *ibid.* **54**, 11169 (1996); G. Kresse and D. Joubert, *ibid.* **59**, 1758 (1999); P. E. Blöchl, *ibid.* **50**, 17953 (1994).
- ²⁹S. L. Dudarev, G. A. Botton, S. Y. Savrasov, C. J. Humphreys, and A. P. Sutton, *Phys. Rev. B* **57**, 1505 (1998).